JACC: CARDIOVASCULAR IMAGING VOL. 6, NO. 6, 2013

ISSN 1936-878X/$36.00
PUBLISHED BY ELSEVIER INC. http://dx.doi.org/10.1016/j.jcmg.2013.02.006

# OCT Analysis in Patients With Very Late Stent Thrombosis

Soo-Jin Kang, MD,* Cheol Whan Lee, MD, PHD,* Haegeun Song, MD,* Jung-Min Ahn, MD,* Won-Jang Kim, MD,* Jong-Young Lee, MD,* Duk-Woo Park, MD, PHD,* Seung-Whan Lee, MD, PHD,* Young-Hak Kim, MD, PHD,* Gary S. Mintz, MD,† Seong-Wook Park, MD, PHD,* Seung-Jung Park, MD, PHD*

*Seoul, Korea; and New York, New York*

**OBJECTIVES** We report optical coherence tomography (OCT) findings in 33 patients who presented with very late stent thrombosis (VLST) after either drug-eluting stent (DES) or bare-metal stent (BMS) implantation.

**BACKGROUND** VLST is a potentially life-threatening complication, but the underlying mechanisms remain unclear.

**METHODS** In 33 patients (27 DES- and 6 BMS-treated lesions) with definite VLST, OCT images were acquired before either thrombus aspiration or intravascular ultrasonography (IVUS) imaging.

**RESULTS** The median duration from implantation was 61.5 months in the DES group and 109.1 months in the BMS group. In the overall cohort, combining DES and BMS, 94% showed intraluminal thrombi. VLST was associated with in-stent neointimal rupture in 23 patients (70%); 22 had thrombi near the site of neointimal rupture. Stent malapposition was observed in 14 (42%) lesions, but only 9 of them showed thrombi at the site of stent malapposition; moreover, 6 (18%) stented segments with malapposition also had neointimal rupture. Only 2 (6%) lesions had no evidence of neointimal rupture or malapposition. Stent fracture was detected in 3 DES-treated lesions, all with concomitant neointimal rupture. Compared with lesions without neointimal rupture, lesions with neointimal rupture showed a higher frequency of ST-segment elevation myocardial infarction (65% vs. 20%, respectively, $p = 0.040$) as well as a higher peak creatine kinase-myocardial band level (163.1 ng/ml vs. 15.7 ng/ml, respectively, $p = 0.017$).

**CONCLUSIONS** OCT imaging indicated that advanced neoatherosclerosis with neointimal rupture and thrombosis was the most common mechanism of definite VLST and was associated with a high frequency of ST-segment elevation myocardial infarction. (J Am Coll Cardiol Img 2013;6:695–703)


From the *Department of Cardiology, University of Ulsan College of Medicine, Asan Medical Center, Seoul, Korea; and the †Cardiovascular Research Foundation, New York, New York. This study was supported by Korea Healthcare Technology Research and Development Project, Ministry of Health and Welfare, grant A120711 and by the CardioVascular Research Foundation, Seoul, Republic of Korea. Dr. Mintz has received grant support from Boston Scientific, Volcano, and Infraredx; and is a consultant for Boston Scientific, Volcano, Infraredx, and St. Jude. All other authors have reported that they have no relationships relevant to the contents of this paper to disclose.

Manuscript received November 28, 2012; revised manuscript received January 31, 2013, accepted February 7, 2013.

Very late stent thrombosis (VLST) is a catastrophic complication that occurs beyond 1 year from stent implantation with a steady frequency of 0.6% per year thereafter in drug-eluting stents (DES) (1). However, the precise mechanisms of VLST are the subject of debate. Previous pathologic studies report that delayed arterial healing characterized by persistent fibrin deposition and poor endothelialization is the primary substrate of late DES thrombosis (2,3). Studies by Cook et al. (4,5) and a meta-analysis by Hassan et al. (6) suggest that late stent malapposition with expansive vascular remodeling is more frequent after DES implantation than that with bare-metal stent (BMS) implantation and is associated with VLST. An in vivo study by Guagliumi et al. (7) shows that optical coherence tomography (OCT) detected uncovered stent struts are independently associated with late DES thrombosis. Finally, de novo in-stent neoatherosclerosis induced by chronic inflammation and abnormal vascular responses has been suggested as an additional mechanism of VLST (8–10).

**ABBREVIATIONS AND ACRONYMS**

**BMS** = bare-metal stent(s)

**DES** = drug-eluting stent(s)

**EEM** = external elastic membrane

**IQR** = interquartile range

**IVUS** = intravascular ultrasonography

**MLA** = minimal lumen area

**OCT** = optical coherence tomography

**STEMI** = ST-segment elevation myocardial infarction

**TCFA** = thin-cap fibroatheroma

**VLST** = very late stent thrombosis

We previously reported grayscale intravascular ultrasonography (IVUS) findings of VLST suggesting that stent malapposition was unique to DES-related VLST, while in-stent neointimal rupture was found in both BMS and DES with VLST (8). However, grayscale IVUS is limited both in its ability to characterize the neointima and to accurately identify uncovered stent struts, stent coverage, or stent–vessel wall malapposition. Thus, we report high-resolution OCT findings in 33 patients who presented with VLST.

## METHODS

**Subjects.** From February 2009 to September 2011, a total of 55 consecutive patients (36 DES and 19 BMS lesions) presented with definite VLST (beyond 1 year after stent placement) at the Asan Medical Center, Seoul, Korea. Angiographic evidence of definite stent thrombosis was based on Academic Research Consortium criteria (11). Furthermore, we included only those patients presenting with acute myocardial infarction or patients presenting with unstable angina who had stent thrombosis documented by thrombectomy. Exclusion criteria were hemodynamic instability, balloon pre-dilation, or thrombectomy prior to OCT examination; inability of the OCT ImageWire or DragonFly catheter (LightLab Imaging, Inc., Westford, Massachusetts) to cross the lesion into the distal vessel due to tight stenosis or severe tortuousity; or presence of left main lesions or saphenous vein graft lesions. In addition, before April 2011, OCT examination using the proximal occlusive technique could not be carried out in lesions located near the ostium. Thus, OCT imaging was performed with 36 patients. After excluding 3 patients whose image quality was poor, we included 33 patients with 33 VLST lesions (27 DES and 6 BMS) in the current study. The DES-VLST group included 22 lesions with the Cypher stent (Cypher Select, Cordis, Johnson & Johnson, Miami, Florida), 3 with Taxus stents (Boston Scientific Corp., Natick, Massachusetts), 1 with Xience stent (Abbot Vascular, Santa Clara, California), and 1 with Pico Elite stent (amg International GmbH, Raesfeld-Erle, Germany). Baseline C-reactive protein was measured before the procedure. All patients signed written informed consent prior to the study.

**Angiographic analysis.** Qualitative and quantitative angiographic measurements were taken using standard techniques with automated edge detection algorithms (CAAS-5, Pie-Medical, Maastricht, the Netherlands) in the angiographic analysis center of the CardioVascular Research Foundation, Seoul, Korea (12).

**OCT imaging and analysis.** All OCT images were acquired before thrombus aspiration or IVUS imaging. Before April 2011, OCT images were acquired using the proximal occlusive technique, the 0.019-inch ImageWire, and a commercially available system (LightLab Imaging, Inc.). The artery was cleared of blood by continuous flushing with iodixanol 370 (Visipaque, GE Health Care, Cork, Ireland) at a flow rate of 3.0 ml/s (13). Since April 2011, OCT images have been acquired using a nonocclusive technique with the C7XR system (LightLab Imaging, Inc.).

Strut-level OCT analysis was performed every 3 frames (every 0.45 mm in images obtained at 3 mm/s pullback using the occlusive technique or every 0.55 mm in images obtained at 20 mm/s pullback using the nonocclusive technique).

Struts were classified as uncovered when a tissue layer on the endoluminal surface was not visible. Struts were classified as malapposed if the distance from the endoluminal surface of the strut to the adjacent lumen contour was greater than the sum of the metal and polymer thickness, not related to a side branch. Thus, the cutoff points of malapposition used for each stent type were 130 μm for the Taxus paclitaxel-eluting stent; 160 μm for the

Cypher sirolimus-eluting stent; and 90 μm for the Xience everolimus-eluting stent (14). To evaluate the distribution of the uncovered (or malapposed) struts, we calculated the proportion of frames with at least one uncovered (or malapposed) strut for each stented segment.

Neointima was the tissue between the luminal border and the inner border of the struts. Calcific intima had a well-delineated, signal-poor region with sharp borders (15). A microvessel (evidence of neovascularization) was defined as a small vesicular or tubular structure with a diameter of ≤200 μm (16). Thin-cap fibroatheroma (TCFA)-containing intima had a fibrous cap thickness of ≤65 μm at the thinnest part, and an angle of ≥180° of lipidic tissue was defined as a signal-poor region with diffuse borders (17–19). OCT neointimal rupture was a break in the fibrous cap of the neointima so that the lumen was connected with the underlying ruptured cavity; this definition is analogous to that of plaque rupture seen in native atherosclerotic plaques, as has been reported previously (19,20).

Thrombi were masses of ≥250 μm in diameter protruding into the lumen and discontinuous from the surface of the vessel wall. Red thrombi had high backscattering with signal-free shadowing; and white thrombi were signal-rich and had low backscattering (21,22). Thrombus-associated neointimal rupture was located within 5 mm from the thrombus. Similarly, thrombus-associated malapposition was located within 5 mm from the thrombus.

When attenuation caused by large amounts of red thrombus obscured underlying neointima morphology; OCT-detectable TCFA-containing neointima, neointima rupture, or malapposition were identified proximal or distal (or opposite) to the red thrombus. All reported OCT parameters required the agreement of two observers (S.-J.K. and G.S.M.). Examples are shown in Figure 1.

**IVUS imaging and analysis.** IVUS imaging was performed after OCT image acquisition and after intracoronary administration of 0.2 mg of nitroglycerin, using a motorized transducer pullback (0.5 mm/s) and a commercial scanner (Boston Scientific/SCIMED, Minneapolis, Minnesota) consisting of a rotating 40-MHz transducer within a 3.2-F imaging sheath. Using computerized planimetry (EchoPlaque version 3.0 software, Indec Systems, MountainView, California), stent and reference segments were assessed. Measurements included external elastic membrane (EEM) area, stent area, and minimal lumen area (MLA). Neointimal rupture and stent malapposition were defined as described above (8,19,20).

**Statistical analysis.** All statistical analyses were performed using SPSS software version 10.0 (SPSS Inc., Chicago, Illinois). All values are expressed as the median value (interquartile range [IQR]) or as counts and percentages (categorical variables). Continuous variables were compared by use of the nonparametric Mann-Whitney test; categorical variables were compared with chi-square statistics or the Fisher exact test. A p value $<0.05$ was considered statistically significant. Comparisons of continuous variables among three groups were performed with the Kruskal-Wallis test. Bonferroni corrections were made for multiple comparisons of continuous variables. All p values after Bonferroni correction of $<0.05$ were considered statistically significant.

## RESULTS

**Baseline clinical and procedural characteristics.** The clinical and procedural characteristics of the 33 patients with definite VLST are summarized in Table 1. The clinical presentation was ST-segment elevation myocardial infarction (STEMI) in 17 (52%), non–ST-segment elevation myocardial infarction (NSTEMI) in 11 (33%), and unstable angina (with documented thrombus) in 5 (15%). The median follow-up time was 74.1 months (IQR: 45.9 to 90.4 months), overall 61.5 months (IQR: 38.7 to 80.3 months) in 27 DES-treated lesions and 109.1 months (IQR: 93.7 to 135.6 months) in 6 BMS-treated lesions. DES-VLST was related to recent withdrawal of dual antiplatelet therapy in 1 patient. Angiographic and IVUS data are shown in Table 2.

**Thrombi, TCFA, and neointimal rupture.** OCT findings are summarized in Table 3. Overall, 31 (94%) lesions showed intraluminal thrombi (93% in DES lesions vs. 100% in BMS lesions, $p = 0.665$). Combining DES and BMS values, red thrombi were observed in 26 (79%) and white thrombi were seen in 31 (94%) VLST lesions. In the 2 lesions without OCT-detected thrombi, initial angiography showed haziness, and in both lesions, OCT showed abundant neointima and intimal rupture at the MLA site without abnormal OCT findings of the reference segments.

In the overall cohort, combining DES and BMS, neointimal rupture was seen in 23 (70%): 17 lesions with single ruptures and 6 lesions with multiple ruptures; TCFA-containing neointima was seen in 21 (64%). The relationship between the site of the TCFA-containing neointima or site of neointimal rupture and the MLA site was shown in Table 3.

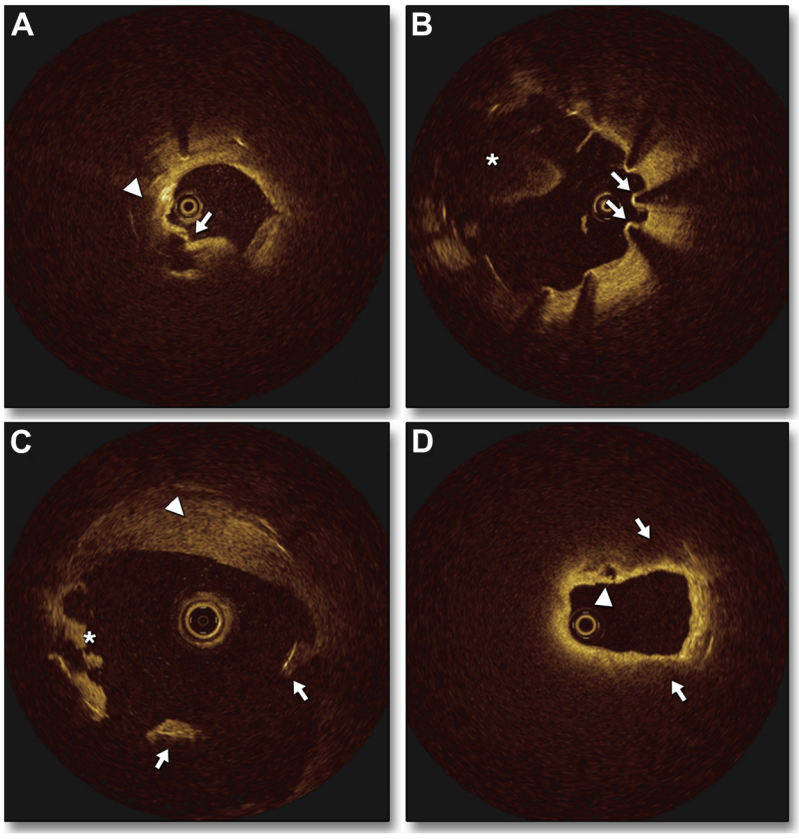


**Figure 1. OCT Findings in Patients With VLST**

**(A)** A 69-year-old male who underwent bare-metal stent (BMS) implantation into the proximal left anterior descending artery presented with ST-segment elevation myocardial infarction (STEMI) 165 months later. There was in-stent intimal rupture **(arrow)** within underlying lipidic tissue **(arrowhead)**. **(B)** A 51-year-old male presented with STEMI 75 months after Cypher stent placement. A lack of neointimal tissue, and malapposed struts **(arrows)**, and red thrombi **(asterisk)** were found at the same frame. **(C)** A very large area of malapposition **(arrows)** with expansive remodeling and mural thrombus **(arrowhead)** was found in a 69-year-old male with non–ST-segment elevation myocardial infarction (NSTEMI) 53 months after Cypher stent implantation. Small white thrombi **(asterisk)** were associated with malapposed stent struts. **(D)** A 79-year-old male presented with NSTEMI 60 months after Cypher stent implantation. There were intimal ruptures **(arrowhead)** and underlying thin-cap fibroatheroma (TCFA)-containing neointima **(arrows)**. There were no malapposed struts.

**Stent strut coverage and malapposition.** Table 3 summarizes stent strut tissue coverage and malapposition assessed by OCT. In the DES-treated lesions 15 (56%) had at least 1 frame with uncovered struts, and 14 (52%) had at least 1 frame with malapposed struts. Conversely, in the BMS group, all but one lesion showed completely covered stent struts.

**Mechanisms of VLST.** In the overall cohort combining DES and BMS, VLST was associated with in-stent neointimal rupture in 23 (70%) lesions (Fig. 2A); all but one had thrombi near the site of the ruptured neointima. Stent malapposition was observed in 14 (42%) lesions, but only 9 (64%) of them showed thrombi within the malapposed segments; moreover, 6 (18%) lesions with malapposition also had neointimal rupture within the stented segment. Only 2 (6%) lesions had no evidence of neointimal rupture or malapposition.

In 27 DES with VLST, neointimal rupture was seen in 17 (63%) and malapposition was seen in 14 (52%); both neointimal rupture and malapposition were seen in 6 (22%). All of the 6 BMS with VLST lesions showed in-stent neointimal rupture without malapposition.

Stent fracture was detected in 3 Cypher-treated lesions. All of the lesions showed abundant neointima containing a TCFA and intimal rupture near the stent fracture. Although expansive remodeling was seen in all of these lesions, only 1 was associated with malapposition of a minimal degree.

**Clinical correlations.** Compared with lesions without neointimal rupture, lesions with neointimal

**Table 1. Baseline Clinical and Procedural Characteristics**

| | No. of Patients With DES, % (n = 27) | No. of Patients With BMS, % (n = 6) | p Value |
|---|---|---|---|
| Age, yrs | 57.0 (52.0–73.0) | 70.0 (60.7–73.3) | 0.260 |
| Male | 23 (85) | 5 (83) | 0.660 |
| Smoking | 17 (63) | 2 (33) | 0.192 |
| Hypertension | 16 (59) | 4 (67) | 0.558 |
| Hypercholesterolemia | 19 (70) | 4 (67) | 0.605 |
| Diabetes mellitus | 9 (33) | 1 (17) | 0.395 |
| Statin therapy at admission | 15 (56) | 3 (50) | 0.934 |
| Previous MI | 7 (26) | 9 (0) | |
| Stent duration, months | 61.5 (38.7–80.3) | 109.1 (93.7–135.6) | <0.001 |
| Antiplatelet therapy | | | |
| No antiplatelet agent | 3 (11) | 2 (33) | 0.208 |
| Aspirin | 18 (67) | 3 (50) | |
| Aspirin + Clopidogrel | 3 (11) | 1 (17) | |
| Aspirin + Cilostazol | 1 (4) | 0 (0) | |
| No information | 2 (7) | 0 (0) | |
| LDL-cholesterol, mg/dl | 80.0 (64.0–99.0) | 101.5 (77.5–174.8) | 0.173 |
| Baseline C-reactive protein, mg/dl* | 0.10 (0.10–0.24) | 0.10 (0.10–0.14) | 0.127 |
| Baseline CK-MB, ng/ml† | 4.5 (1.0–9.0) | 1.1 (1.0–42.5) | 0.569 |
| Peak CK-MB, ng/ml† | 92.0 (10.6–302.3) | 77.5 (8.6–209.7) | 0.398 |
| Total stent length, mm | 31.5 (23.0–43.1) | 24.3 (17.3–26.9) | 0.065 |

Values are n (range) or n (%). Median values (interquartile ranges) were compared using a nonparametric Mann-Whitney test. p values are DES versus BMS. *CRP was measured in 18 patients before the procedure. †Normal reference value of CK-MB: 0–5.0 ng/ml.
BMS = bare-metal stent(s); CK-MB = creatine kinase-myocardial band; DES = drug-eluting stent(s); LDL = low-density lipoprotein; MI = myocardial infarction.

rupture showed a higher frequency of STEMI (65% vs. 20%, respectively, p = 0.040) as well as a higher peak creatine kinase-myocardial band (CK-MB) (163.1 ng/ml [IQR: 21.2 to 302.3 ng/ml] vs. 15.7 ng/ml [IQR: 4.4 to 66.4 ng/ml], respectively, p = 0.017). Furthermore, a TIMI flow grade of 3 was less frequent in lesions with neointimal rupture than in those without neointimal rupture (22% vs. 63%, respectively, p = 0.044). All 3 patients with Cypher stent fracture and VLST presented with STEMI. Figure 2B compares the major OCT findings between 17 patients who presented with STEMI and 16 patients who presented with NSTEMI or unstable angina (with documented thrombus).

## DISCUSSION

In-stent neoatherosclerosis has been reported as a mechanism of both DES and BMS failure although it occurs earlier in DES-treated lesions than in BMS-treated lesions (9). Unstable characteristics such as in-stent TCFA and neointimal rupture have been associated with late thrombotic events both in vitro and in vivo (9,16,18,23–25). The major findings of the current report are: 1) all BMS with VLST showed in-stent neointimal rupture without malapposition, consistent with previous data (8,23,24). 2) In DES with VLST, the frequency of neointimal rupture was 63%; and the frequency of malapposition was 52%. However, both malapposition and neointimal rupture were seen in 22%; and thrombi were more often associated with neointimal rupture than with malapposition. 3) Compared with lesions without neointimal rupture, patients with neointimal rupture showed a higher frequency of STEMI with slow flow and a higher peak CK-MB at the time of presentation of VLST.

Unlike BMS-treated lesions with VLST, VLST after DES implantation is multifactorial in causality and varies among the many publications. Cook et al. (4) demonstrated incomplete stent apposition in 77% of patients with VLST, especially a larger malapposition area. In another analysis of thrombus aspirates from patients who presented with VLST, findings suggested that hypersensitivity was a cause

**Table 2. Angiographic and Intravascular Ultrasound Data**

| | No. of Patients With DES, % (n = 27) | No. of Patients With BMS, % (n = 6) | p Value |
|---|---|---|---|
| Angiographic findings | | | |
| Lesion location | | | |
| Left anterior descending | 17 (63) | 4 (67) | 0.855 |
| Left circumflex | 2 (7) | 0 (0) | |
| Right coronary | 7 (26) | 2 (33) | |
| Ramus intermedius | 1 (4) | 0 (0) | |
| Proximal reference diameter, mm | 3.9 (3.5–4.3) | 3.6 (3.3–3.8) | 0.132 |
| Distal reference diameter, mm | 2.5 (2.3–3.2) | 2.9 (2.4–3.0) | 0.862 |
| Minimal lumen diameter, mm | 0.0 (0.0–0.9) | 0.0 (0.0–1.2) | 0.910 |
| Diameter stenosis | 100.0 (74.0–100.0) | 100.0 (60.0–100.0) | 0.982 |
| TIMI flow grade | | | |
| TIMI 0 | 12 (44) | 2 (33) | 0.698 |
| TIMI 1 | 4 (14.9) | 1 (17) | |
| TIMI 2 | 3 (11) | 0 (0) | |
| TIMI 3 | 8 (30) | 3 (50) | |
| Stent fracture | 3 (11) | 0 (0) | 0.693 |
| Intravascular ultrasound findings | | | |
| Proximal reference lumen area, $mm^2$ | 5.4 (3.4–8.3) | 7.1 (4.1–9.8) | 0.440 |
| Proximal reference EEM area, $mm^2$ | 16.8 (12.9–19.7) | 17.5 (10.1–20.2) | 0.859 |
| Distal reference lumen area, $mm^2$ | 3.4 (2.4–4.4) | 2.8 (1.8–3.6) | 0.309 |
| Distal reference EEM area, $mm^2$ | 8.4 (6.9–10.3) | 10.1 (7.1–14.6) | 0.427 |
| Minimal stent area, $mm^2$ | 5.5 (4.4–7.3) | 7.3 (5.8–9.0) | 0.093 |
| MLA, $mm^2$ | 1.7 (1.3–2.2) | 1.6 (1.3–1.9) | 0.667 |
| EEM area at the MLA site, $mm^2$ | 17.1 (12.7–22.1) | 15.3 (15.1–17.1) | 0.561 |
| Remodeling index | 1.6 (1.2–2.6) | 1.2 (1.1–1.7) | 0.127 |

Values are n (%) or n (range). Median values (interquartile ranges) were compared using a nonparametric Mann-Whitney test. p values are comparisons of DES versus BMS.
EEM = external elastic membrane; MLA = minimal lumen area; TIMI = Thrombolysis In Myocardial Infarction; other abbreviations as in Table 1.

and was associated with vascular remodeling and secondary stent malapposition (5). Using OCT to study 18 patients with DES-VLST, Hong et al. (26) reported that 22% had intimal rupture, while malapposed struts were found in 50%. More recently, Guagliumi et al. (7) evaluated 18 patients with late or very late DES thrombosis and showed higher frequencies of uncovered (12.2% vs. 4.1%, respectively) and malapposed struts (4.6% vs. 1.8%, respectively), while neointimal rupture was seen in only 17%.

This study is different from previous OCT studies. In the current study we saw neointimal rupture in 63% of DES-VLST lesions. Although 22% showed both neointimal rupture and malapposition, neointimal rupture more likely contributed to the thrombotic event because of the spatial relationship of the intracoronary thrombus to the site of neointimal rupture. There are 2 plausible explanations for the discrepancy between the frequency of neointimal rupture in the current analysis and that in previous reports (7,26). The time between DES implantation and VLST is shorter in previous studies (Hong et al. [26], 40 ± 18 months; Guagliumi et al. [7], median 20.5 months) than in our current study (median 61.5 months). The frequency of in-stent neoatherosclerosis, that is, the precursor for neointimal rupture and VLST, is time dependent and is not a consistent finding until approximately 1.5 to 2.0 years post-DES implantation (9,19). Moreover, in both previous OCT studies, OCT examination had been done after thrombus aspiration, while in the current analysis, OCT had been performed before thrombus aspiration. A recent study by Kimura et al. (27) shows that aspirates from VLST lesions

**Table 3. OCT Findings in Patients With VLST**

| | No. of Patients With DES, % (n = 27) | No. of Patients With BMS, % (n = 6) | p Value |
|---|---|---|---|
| Neovascularization | 11 (41) | 3 (50) | 0.687 |
| OCT-MLA, $mm^2$ | 1.2 (0.8–1.8) | 1.2 (0.9–2.5) | 0.372 |
| OCT-MSA at the MLA site, $mm^2$ | 8.0 (6.5–9.1) | 9.7 (8.3–11.3) | 0.040 |
| OCT-MSA <5.0, $mm^2$ | 2 (7) | 0 (0) | 0.782 |
| Minimum thickness of fibrous cap, μm | 60 (50–120) | 50 (48–52) | 0.040 |
| Intimal rupture | 17 (63) | 6 (100) | 0.074 |
| MLA site | 12 (44) | 3 (50) | 0.805 |
| Proximal to the MLA | 8 (30) | 5 (83) | 0.015 |
| Distal to the MLA | 1 (4) | 0 (0) | 0.632 |
| TCFA-containing neointima | 15 (56) | 6 (100) | 0.041 |
| MLA site | 11 (41) | 3 (50) | 0.678 |
| Proximal to the MLA | 8 (30) | 5 (83) | 0.015 |
| Distal to the MLA | 3 (11) | 2 (33) | 0.170 |
| Total number of OCT-frames | 1,592 | 248 | |
| Proportion of frames with at least 1 | | | |
| Uncovered strut, % | 12.9 ± 15.5 | 0.5 ± 1.3 | 0.072 |
| Malapposed strut, % | 7.8 ± 11.1 | 0.0 ± 0.0 | 0.050 |
| Proportion of lesions with at least 1 | | | |
| Frame with uncovered strut | 15 (56) | 1 (17) | 0.085 |
| Frame with malapposed strut | 14 (52) | 0 (0) | 0.020 |

Values are n (%) or n (range). Continuous variables are presented as median values (interquartile ranges) and were compared using a nonparametric Mann-Whitney test.
MSA = minimal stent area; OCT = optical coherence tomography; TCFA = thin-cap fibroatheroma; other abbreviations as in Table 1.

frequently contain fragments of atherosclerotic intima and thin fibrous cap (27). Thus, the simple protocol decision whether to perform thrombectomy first or OCT first would affect the diagnosis of the cause of VLST and the published findings. Furthermore, because red thrombus may obscure the presence of neointimal rupture or malapposition, the finding of a "vulnerable" neointima might be underestimated (but not overestimated!), unless thrombectomy is performed first. Thus, our study suggests that advanced neoatherosclerosis with neointimal rupture is the primary mechanism of VLST.

Regarding the remaining 37% of VLST lesions without neointimal rupture, despite a high frequency of malapposed struts, it is uncertain whether malapposition is a direct cause of VLST or merely a marker of an underlying pathobiological process as suggested by Cook (4,5). Stent fracture has been associated with peri-stent staining or aneurysmal changes and may be related to late stent thrombosis as well as late catch-up (27–29). However, in all 3 DES VLST lesions with stent fracture in our current study, neointimal rupture within abundant neointima has been documented irrespective of presence of malapposition. This suggests an interrelationship among neoatherosclerosis, restenosis, VLST, and stent fracture in some patients.

Compared with patients with VLST without neointimal rupture, patients with VLST and neointimal rupture more often presented with STEMI and had a higher peak CK-MB. Thus, the underlying mechanism of VLST was as important as the VLST event itself; neointimal rupture was associated with more intense clinical sequelae in the setting of stent thrombosis.

We previously reported the following OCT findings of DES restenosis: TCFA-containing neointima in 52%, neointimal rupture in 58% and intraluminal thrombi in 58%, all evidence of "vulnerable" neointima (19). Unstable clinical presentation was associated with a thinner fibrous cap and a higher frequency of these vulnerable neointima findings. In this report we extend our OCT observations to definite VLST.

**Study limitations.** This was a cross-sectional observational study identifying the mechanisms of VLST, but not the predictive power of OCT in

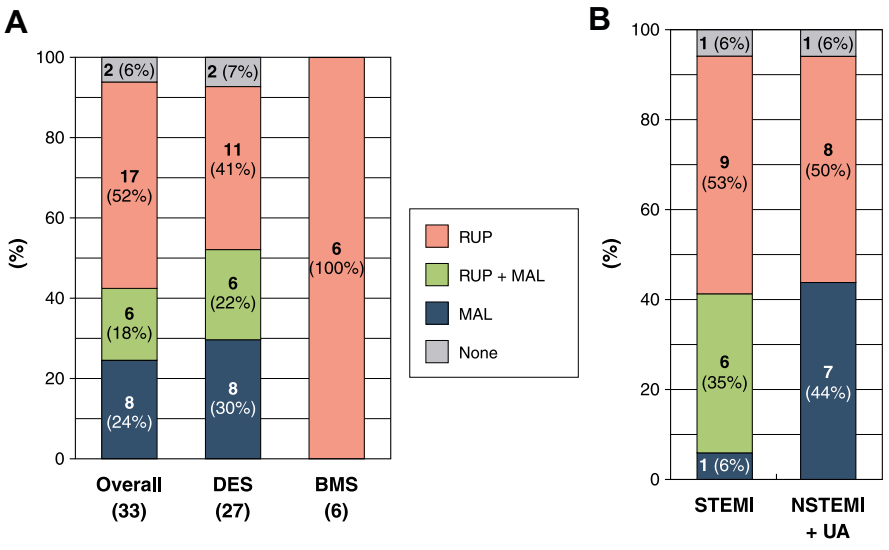


**Figure 2. Frequencies of Malapposition and Intimal Rupture**

**(A)** Frequency of OCT-defined malapposition (MAL) and intimal rupture (RUP). **(B)** Frequency of OCT-defined malapposition and intimal rupture in patients with STEMI versus those with either NSTEMI or unstable angina (UA). DES = drug-eluting stent(s); other abbreviations as in Figure 1.

an asymptomatic population. This study had no control group, and there were no serial OCT or follow-up data. Despite the largest patient cohort with definite VLST reported so far, the sample size was still underpowered to perform any subgroup assessment or multivariable analysis. Because of signal attenuation caused by thrombi, accurate assessment of structures behind massive thrombi was limited. Although underlying plaque morphology potentially affected the mechanisms of VLST, OCT artifacts behind stent struts and shallow penetration limited the assessment of peristent plaque. Finally, OCT images included only in-stent and adjacent reference segments and not far proximal or distal segments.

## CONCLUSIONS

Intracoronary OCT at the time of acute clinical presentation showed that all BMS lesions with VLST and 63% of DES lesions with VLST had in-stent neointimal rupture; and two-thirds of them presented with STEMI, suggesting that advanced neoatherosclerosis was a common and aggressive mechanism of VLST.

**Reprint requests and correspondence:** Dr. Seung-Jung Park, Department of Cardiology, University of Ulsan College of Medicine, Asan Medical Center, 388-1 Poongnap-dong, Songpa-gu, Seoul 138-736, South Korea. *E-mail: sjpark@amc.seoul.kr.*

## REFERENCES

1. Daemen J, Wenaweser P, Tsuchida K, et al. Early and late coronary stent thrombosis of sirolimus-eluting and paclitaxel-eluting stents in routine clinical practice: data from a large two-institutional cohort study. Lancet 2007;369:667–78.
2. Joner M, Finn AV, Farb A, et al. Pathology of drug-eluting stents in humans: delayed healing and late thrombotic risk. J Am Coll Cardiol 2006;48:193–202.
3. Nakazawa G, Finn AV, Joner M, et al. Delayed arterial healing and increased late stent thrombosis at culprit sites after drug-eluting stent placement for acute myocardial infarction patients: an autopsy study. Circulation 2008;118:1138–45.
4. Cook S, Wenaweser P, Togni M, et al. Incomplete stent apposition and very late stent thrombosis after drug-eluting stent implantation. Circulation 2007;115:2426–34.
5. Cook S, Ladich E, Nakazawa G, et al. Correlation of intravascular ultrasound findings with histopathological analysis of thrombus aspirates in patients with very late drug-eluting stent thrombosis. Circulation 2009;120:391–9.
6. Hassan AK, Bergheanu SC, Stijnen T, et al. Late stent malapposition risk is higher after drug-eluting stent compared with bare-metal stent implantation and associates with late stent thrombosis. Eur Heart J 2010;31:1172–80.

7. Guagliumi G, Sirbu V, Musumeci G, et al. Examination of the in vivo mechanisms of late drug-eluting stent thrombosis findings from optical coherence tomography and intravascular ultrasound imaging. J Am Coll Cardiol Intv 2012;5:12–20.
8. Lee CW, Kang SJ, Park DW, et al. Intravascular ultrasound findings in patients with very late stent thrombosis after either drug-eluting or bare-metal stent implantation. J Am Coll Cardiol 2010;55:1936–42.
9. Nakazawa G, Otsuka F, Nakano M, et al. The pathology of neoatherosclerosis in human coronary implants bare-metal and drug-eluting stents. J Am Coll Cardiol 2011;57:1314–22.
10. Joner M, Nakazawa G, Finn AV, et al. Endothelial cell recovery between comparator polymer-based drug-eluting stents. J Am Coll Cardiol 2008;52:333–42.
11. Cutlip DE, Windecker S, Mehran R, et al., for the Academic Research Consortium. Clinical end points in coronary stent trials: a case for standardized definitions. Circulation 2007;115:2344–51.
12. Ryan TJ, Faxon DP, Gunnar RM, et al. Guidelines for percutaneous transluminal coronary angioplasty. A report of the American College of Cardiology/American Heart Association Task Force on Assessment of Diagnostic and Therapeutic Cardiovascular Procedures (Subcommittee on Percutaneous Transluminal Coronary Angioplasty). Circulation 1988;78:486–502.
13. Gonzalo N, Garcia-Garcia HM, Regar E, et al. In vivo assessment of high-risk coronary plaques at bifurcations with combined intravascular ultrasound virtual histology and optical coherence tomography. J Am Coll Cardiol Img 2009;2:473–82.
14. Gonzalo N, Barlis P, Serruys PW, et al. Incomplete stent apposition and delayed tissue coverage are more frequent in drug-eluting stents implanted during primary percutaneous coronary intervention for ST-segment elevation myocardial infarction than in drug-eluting stents implanted for stable/unstable angina: insights from optical coherence tomography. J Am Coll Cardiol Intv 2009;2:445–52.
15. Yabushita H, Bouma BE, Houser SL, et al. Characterization of human atherosclerosis by optical coherence tomography. Circulation 2002;106:1640–5.
16. Takano M, Yamamoto M, Inami S, et al. Appearance of lipid-laden intima and neovascularization after implantation of bare-metal stents extended late-phase observation by intracoronary optical coherence tomography. J Am Coll Cardiol 2009;55:26–32.
17. Regar E, van Beusekom HMM, van der Gissen WJ, Serruys PW. Optical coherence tomography findings at 5-year follow-up after coronary stent implantation. Circulation 2005;112:e345–6.
18. Habara M, Terashima M, Nasu K, et al. Difference of tissue characteristics between early and very late restenosis lesions after bare-metal stent implantation: an optical coherence tomography study. Circ Cardiovasc Interv 2011;4:232–8.
19. Kang SJ, Mintz GS, Akasaka T, et al. Optical coherence tomographic analysis of in-stent neoatherosclerosis after drug-eluting stent implantation. Circulation 2011;123:2954–63.
20. Prati F, Regar E, Mintz GS, et al. Expert's OCT Review Document. Expert review document on methodology, terminology, and clinical applications of optical coherence tomography: physical principles, methodology of image acquisition, and clinical application for assessment of coronary arteries and atherosclerosis. Eur Heart J 2010;31:401–15.
21. Kume T, Akasaka T, Kawamoto T, et al. Assessment of coronary arterial thrombus by optical coherence tomography. Am J Cardiol 2006;97:1713–7.
22. Jang IK, Tearney GJ, MacNeill, et al. In vivo characterization of coronary atherosclerotic plaque by use of optical coherence tomography. Circulation 2005;111:1551–5.
23. Hou J, Qi H, Zhang M, et al. Development of lipid-rich plaque inside bare metal stent: possible mechanism of late stent thrombosis? An optical coherence tomography study. Heart 2010;96:1187–90.
24. Yamaji K, Inoue K, Nakahashi T, et al. Bare metal stent thrombosis and in-stent neoatherosclerosis. Circ Cardiovasc Interv 2012;5:47–54.
25. Kang SJ, Mintz GS, Park DW, et al. Tissue characterization of in-stent neointima using intravascular ultrasound radiofrequency data analysis. Am J Cardiol 2010;106:1561–5.
26. Ko YG, Kim DM, Cho JM, et al. Optical coherence tomography findings of very late stent thrombosis after drug-eluting stent implantation. Int J Cardiovasc Imaging 2012;28:715–23.
27. Imai M, Kadota K, Goto T, et al. Incidence, risk factors, and clinical sequelae of angiographic peri-stent contrast staining after sirolimus-eluting stent implantation. Circulation 2011;123:2382–91.
28. Doi H, Maehara A, Mintz GS, et al. Classification and potential mechanisms of intravascular ultrasound patterns of stent fracture. Am J Cardiol 2009;103:818–23.
29. Yang TH, Kim DI, Jin HY, et al. "Angiographic late catch-up" phenomenon after sirolimus-eluting stent implantation. Int J Cardiol 2012;160:48–52.

**Key Words:**
neoatherosclerosis ■ optical coherence tomography ■ very late stent thrombosis.